Electronic Supplementary Material (ESI) for Inorganic Chemistry Frontiers.

Supporting Information for

Experimental and Theoretical Study of $LuNC@C_{76,82}$ Revealing a Cage-cluster Selection Rule

Wangqiang shen,‡[a] Ziqi Hu,‡[b] Pengwei Yu,‡[a] Zhan Wei,[c] Peng Jin,*[c] Zujin Shi *[b] and Xing Lu*[a]

[a]*State Key Laboratory of Materials Processing and Die & Mould Technology, School of Materials Science and Engineering, Huazhong University of Science and Technology, 1037 Luoyu Road, Wuhan, 430074 China. E-mail: lux@hust.edu.cn.*

[b]*State Key Laboratory of Rare Earth Materials Chemistry and Applications, Beijing Key Laboratory for Magnetoelectric Materials and Devices, College of Chemistry and Molecular Engineering, Peking University, Beijing 100871, P. R. China. E-mail: zjshi@pku.edu.cn.*

[c]*School of Materials Science and Engineering, Hebei University of Technology, Tianjin, 300130 China. E-mail: china.peng.jin@gmail.com.*

Separation steps of $LuC_{77}N$, $LuC_{83}N$-I, $LuC_{83}N$-II, and $LuC_{83}N$-III samples. First, the toluene solution of the extract was separated by using LC-9130NEXT apparatus monitored using a UV detector at 330 nm and a Buckyprep column (20 mm × 250 mm, Cosmosil Nacalai Tesque) with toluene as the mobile phase, and fraction 1 was collected (Figure. S1a). Then, fraction 1 was reinjected into a Buckyprep M column (20 mm × 250 mm, Cosmosil Nacalai Tesque) for the next separation using toluene as the eluent, and fraction 1-1 was obtained (Figure S1b). Fraction 1-1 was then carried out on a 5PYE column (20 mm × 250 mm, Cosmosil Nacalai Tesque) with toluene as the mobile phase, and fraction 1-1-1 was obtained (Figure S2a). Fraction 1-1-1 was then reinjected into a 5PYE column (20 mm × 250 mm, Cosmosil Nacalai Tesque) for the next separation using toluene as the eluent, and fraction 1-1-1-1 was obtained (Figure S2b). Finally, fraction 1-1-1-1 was reinjected into a Buckyprep column (20 mm × 250 mm, Cosmosil Nacalai Tesque) with toluene as the mobile phase, fractions $LuC_{77}N$ (LuNC@C_{2v}(19138)-C_{76}), $LuC_{83}N$-I (LuNC@C_s(6)-C_{82}), $LuC_{83}N$-II (LuNC@C_{2v}(9)-C_{82}), and $LuC_{83}N$-III (LuNC@C_2(5)-C_{82}) were collected (Figure S2c).

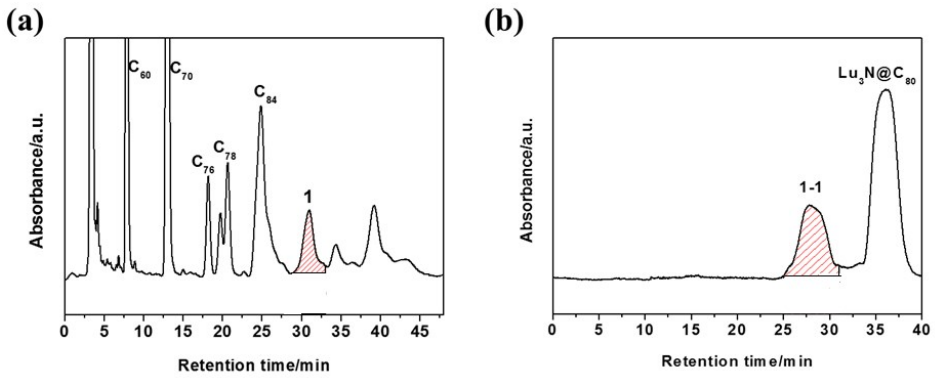

Figure S1. (a) Chromatogram of the fullerene extract mixture synthesized from Lu_2O_3 with addition of N_2 (20 mm × 250 mm Buckyprep column; flow rate 10 mL/min; injection volume 20 ml; toluene as eluent; room temperature). (b) Chromatogram of fraction 1 (20 mm × 250 mm Buckyprep M column; flow rate 10 mL/min; injection volume 20 ml; toluene as eluent; room temperature).

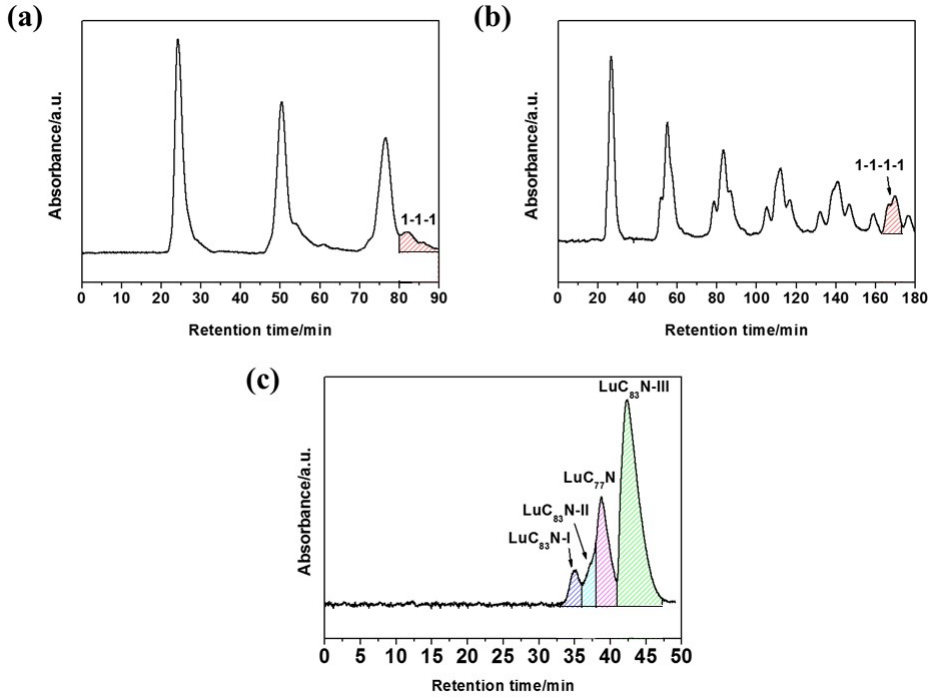

Figure S2. (a) Chromatogram of fraction 1-1 (20 mm × 250 mm 5PYE column; flow rate 10 mL/min; injection volume 20 ml; toluene as eluent; room temperature). (b) Chromatogram of fraction 1-1-1 (20 mm × 250 mm 5PYE column; flow rate 10 mL/min; injection volume 20 ml; toluene as eluent; room temperature). (c) Chromatogram of fraction 1-1-1-1 (20 mm × 250 mm Buckyprep column; flow rate 10 mL/min; injection volume 20 ml; toluene as eluent; room temperature).

Table S1. The weight of the raw soot and the isolated $Lu_3N@C_{80}$ of every carbon rod.

Component	**Weight**				
raw soot	4.1252 g	4.2334 g	4.0381 g	4.3065 g	4.2587 g
$Lu_3N@C_{80}$	0.0042 g	0.0046 g	0.0039 g	0.0043 g	0.0045 g

The average yield of $Lu_3N@C_{80}$ to the raw soot is: 1/5 × (0.0048/4.1252 + 0.0051/4.2334 + 0.0044/4.0381 + 0.0052/4.3065 + 0.0050/4.2587 = 0.12 %

Table S2. Assignments of each (sub) fraction and their relative abundances.

Fraction	Major component	Relative abundance
1	$Lu_3N@C_{80}$	73.9%
	C_{86}, $Lu_2@C_{76}$, $Lu_2@C_{78}$, $LuC_{77}N$, $LuC_{83}N$	26.1%
1-1	C_{86}	86.3%
	$Lu_2@C_{76}$, $Lu_2@C_{78}$, $LuC_{77}N$, $LuC_{83}N$	13.7%
1-1-1	$Lu_2@C_{76}$, $Lu_2@C_{78}$,	47.4%
	$LuC_{77}N$,$LuC_{83}N$	52.6%
1-1-1-1	LuNC@C_{2v}(19138)-C_{76}	23.8%
	LuNC@C_s(6)-C_{82}	13.6%
	LuNC@C_{2v}(9)-C_{82}	13.0%
	LuNC@C_2(5)-C_{82}	49.6%

(1) The yield of LuNC@C_{2v}(19138)-C_{76} is: 23.8% × 52.6% × 13.7% × 26.1% × 0.12% / 73.9% = 0.00073%

(2) The yield of LuNC@C_s(6)-C_{82} is: 13.6% × 52.6% × 13.7% × 26.1% × 0.12% / 73.9% = 0.00042%

(3) The yield of LuNC@C_{2v}(9)-C_{82} is: 13.0% × 52.6% × 13.7% × 26.1% × 0.12% / 73.9% = 0.00040%

(4) The yield of LuNC@C_2(5)-C_{82} is: 49.6% × 52.6% × 13.7% × 26.1% × 0.12% / 73.9% = 0.00151%

Table S3. Characteristic absorption data of $LuC_{77}N$, $LuC_{83}N$-I, $LuC_{83}N$-II, $LuC_{83}N$-III, and other reported C_{76}- and C_{82}-based CYCFs.

EMFs	Absorption peaks (nm)	Absorption onset (nm)	Optical bandgap (eV)[a]	Reference
$LuC_{77}N$	461, 710, 848, 926, 1162	1338	0.93	This work
TbNC@C_{2v}(19138)-C_{76}	469, 702, 843, 936, 1049, 1182	1314	0.94	[S1]
YNC@C_{2v}(19138)-C_{76}	478, 527, 572, 695, 840, 946, 1051, 1185	1302	0.95	[S1]
$LuC_{83}N$-I	494, 596, 744, 1069, 1131, 1345	1638	0.76	This work
TbNC@C_s(6)-C_{82}	389, 491, 741, 1064, 1123, 1318	1620	0.77	[S2]
$LuC_{83}N$-II	512, 621, 697, 782, 1096, 1296	1680	0.74	This work
TbNC@C_{2v}(9)-C_{82}	518, 618, 710, 772, 1144, 1320	1770	0.70	[S2]
$LuC_{83}N$-III	631, 662, 764, 941, 1062	1242	1.00	This work
TbNC@C_2(5)-C_{82}	627, 656, 763, 923, 1056	1240	1.00	[S2]

[a]Optical bandgap (eV) ≈ 1240/onset (eV)

Table S4. Crystallographic data of LuNC@C_{2v}(19138)-C_{76} and LuNC@C_2(5)-C_{82}.

	LuNC@C_{2v}(19138)-C_{76}•Ni^{II}(OEP)•($CHCl_3$)	**LuNC@C_2(5)-C_{82}•Ni^{II}(OEP)•($CHCl_3$)**
T, K	100(2)	100(2)
λ, Å	0.65250	0.65250
color/habit	black / block	black / block
cryst size, mm	0.04×0.02×0.02	0.08×0.06×0.04
empirical formula	$C_{114}H_{37}Cl_3LuN_5Ni$	$C_{120}H_{37}Cl_3LuN_5Ni$
fw	1816.51	1888.57
cryst system	monoclinic	monoclinic
space group	C2/m	C2/m
a, Å	23.481(5)	23.260(5)
b, Å	13.973(5)	14.216(5)
c, Å	17.415(5)	18.082(5)
α, deg	90	90
β, deg	92.819(5)	93.790(5)
γ, deg	90	90
V, $Å^3$	5707(3)	5966(3)
Z	4	4
ρ, g/cm^3	2.114	2.103
μ, mm^{-1}	1.806	1.732
R1 (all data)	0.1766	0.1117
wR2 (all data)	0.3638	0.3053

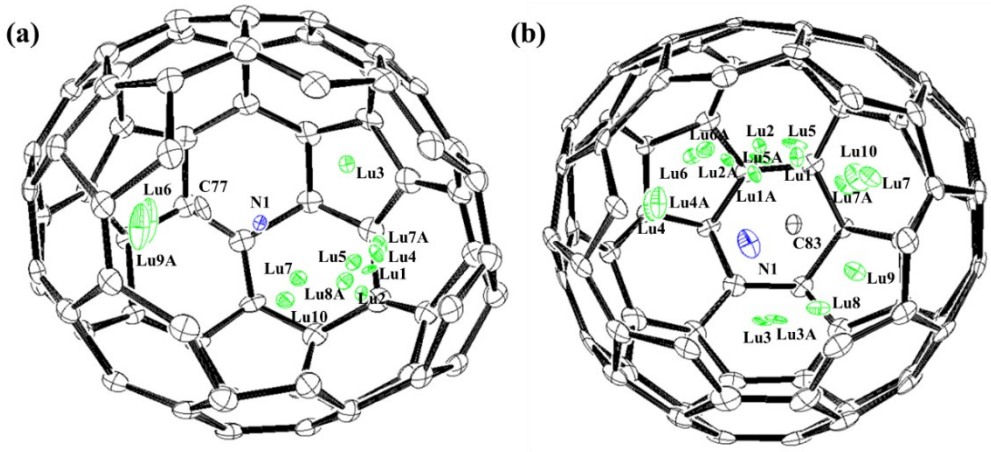

Figure S3. Positions of the disordered lutetium sites in (a) LuNC@C_{2v}(19138)-C_{76} and (b) LuNC@C_2(5)-C_{82} relative to a cage orientation. Those Lu atoms labeled with an "A" are generated by crystallographic operation. Some cage carbon atoms are omitted for clarity.

Table S5. The fractional occupancies of the Lu positions in LuNC@C_{2v}(19138)-C_{76} and LuNC@C_2(5)-C_{82}.

EMFs	**Fractional occupancy of the Lu positions**									
LuNC@C_{2v}(19138)-C_{76}	Lu4	Lu5	Lu6	Lu7	Lu1	Lu2	Lu3			
	0.14	0.05	0.04	0.02	0.42	0.06	0.02			
	Lu4A	Lu5A	Lu6A	Lu7A						
	0.14	0.05	0.04	0.02						
LuNC@C_2(5)-C_{82}	Lu1	Lu2	Lu3	Lu4	Lu5	Lu6	Lu7	Lu8	Lu9	Lu10
	0.17	0.09	0.08	0.03	0.03	0.02	0.01	0.10	0.02	0.02
	Lu1A	Lu2A	Lu3A	Lu4A	Lu5A	Lu6A	Lu7A			
	0.17	0.09	0.08	0.03	0.03	0.02	0.01			

Table S6. Calculated Wiberg bond order (WBO), electron occupancies (Occ., e), hybrid composition, and natural population analysis (NPA) charges of the single crystals of LuNC@C_{2v}(19138)-C_{76} and LuNC@C_2(5)-C_{82}.

Compound	WBO	Bond	Occ.	Hybrid composition	Atom	Charge
LuNC@C_{2v}(19138)-C_{76}	C-N 2.92	C-N	1.98	C s(33%)p(67%) N s(61%)p(39%)	C	+0.25
		C-N	1.93	C p(100%) N p(100%)	N	-0.90
		C-N	1.93	C p(100%) N p(100%)	Lu	+1.45
LuNC@C_2(5)-C_{82}	C-N 2.86	C-N	1.97	C s(27%)p(73%) N s(41%)p(59%)	C	+0.22
		C-N	1.96	C s(7%) p(93%) N s(12%)p(88%)	N	-0.67
		C-N	1.94	C p(100%) N p(100%)	Lu	+1.37

Table S7. Density descriptors (unit: au) at the BCPs for LuNC@C_{2v}(19138)-C_{76} and LuNC@C_2(5)-C_{82}.

Compound	BCP	ρ_{BCP}	$\nabla^2\rho_{BCP}$	H_{BCP}	$\lvert V_{BCP}\rvert / G_{BCP}$	G_{BCP}/ρ_{BCP}
LuNC@C_{2v}(19138)-C_{76}	C-N	0.453	0.018	-0.806	2.006	1.768
	Lu-N	0.087	0.346	-0.019	1.177	1.200
	N-C1	0.003	0.011	0.000	0.836	0.714
	N-C2	0.003	0.011	0.000	0.820	0.697
	Lu-C3	0.045	0.160	-0.004	1.090	0.970
	Lu-C4	0.057	0.201	-0.009	1.153	1.033
	Lu-C5	0.057	0.201	-0.009	1.152	1.035
	Lu-C6	0.045	0.160	-0.004	1.087	0.971
	C-C7	0.009	0.032	0.001	0.799	0.748
	C-C8	0.009	0.032	0.001	0.798	0.747
LuNC@C_2(5)-C_{82}	C-N	0.456	0.013	-0.816	1.996	1.795
	Lu-N	0.068	0.269	-0.009	1.121	1.132
	C-C1	0.003	0.010	0.000	0.806	0.586
	Lu-C2	0.051	0.158	-0.007	1.147	0.915
	Lu-C3	0.060	0.187	-0.011	1.185	0.965
	Lu-C4	0.060	0.185	-0.011	1.190	0.956
	N-C5	0.003	0.011	0.000	0.818	0.721
	N-C6	0.003	0.011	0.000	0.808	0.706
	C-C7	0.006	0.020	0.001	0.765	0.652

References:

[S1] F. Liu, S. Wang, C.-L. Gao, Q. Deng, X. Zhu, A. Kostanyan, R. Westerström, F. Jin, S.-Y. Xie, A.A. Popov, T. Greber, and S. Yang, Mononuclear Clusterfullerene Single-Molecule Magnet Containing Strained Fused-Pentagons Stabilized by a Nearly Linear Metal Cyanide Cluster, *Angew. Chem. Int. Ed.*, 2017, **56**, 1830–1834.

[S2] F. Liu, C.-L. Gao, Q. Deng, X. Zhu, A. Kostanyan, R. Westerström, S. Wang, Y.-Z. Tan, J. Tao, S.-Y. Xie, A.A. Popov, T. Greber, and S. Yang, Triangular Monometallic Cyanide Cluster Entrapped in Carbon Cage with Geometry-Dependent Molecular Magnetism, *J. Am. Chem. Soc.*, 2016, **138**, 14764–14771.